The Role of Boron in TiAl Alloy Development – A Review

Hu, Dawei

DOI:
10.1007/s12598-015-0615-1

Document Version
Peer reviewed version

Citation for published version (Harvard):
Hu, D 2016, 'The Role of Boron in TiAl Alloy Development – A Review', *Rare Metals*, vol. 35, no. 1, pp. 1-14. https://doi.org/10.1007/s12598-015-0615-1

The Role of Boron in TiAl Alloy Development – A Review

Dawei Hu (0000-0003-0718-2663)

Interdisciplinary Research Centre in Materials, The University of Birmingham,
Edgbaston, Birmingham, B15 2TT, UK
Email: d.hu@bham.ac.uk

Abstract Boron was found to be a unique grain refiner in cast TiAl alloys in the beginning of 1990s and has become an element in most of the TiAl alloys developed to date. Over the past 25 or so years efforts to understand the role of boron in solidification, solid phase transformation, thermal and thermomechanical processing and mechanical properties of TiAl alloys and the relevant mechanisms never ceased. As a result, abundant knowledge on boron in TiAl alloys has been accumulated but scattered in various research papers and conference proceedings. This review summarises the progress in understanding boron and its impacts to the TiAl alloy systems.

Keywords Titanium aluminide, TiAl, Ti_3Al, Boron, Grain refinement.

1 Introduction

With the smooth insertion of cast TiAl low pressure turbine (LPT) blades into commercial GEnx engines and the successful test flight of wrought TiAl LPT blades in a geared turbo fan PW1000G engine the fruition of long term TiAl development in aero-engine industries is heralded after a few decades' extensive research [1,2]. A consensus has been reached that for application the TiAl alloys must have refined microstructures by whatever means, except for the cases of directional solidification [3]. However, it appeared very difficult to obtain fine-grained microstructures in early cast TiAl alloys featuring coarse columnar microstructures. It is in this sense that boron has started to play an important role. Boron refines microstructures of as-cast TiAl without costly post-casting thermal processing. Ever since the beginning of development of engineering TiAl alloys at the end of 1980s and start of 1990s boron has established itself as an almost indispensable alloying element to TiAl alloys and nowadays most TiAl alloys, whether in cast form or in wrought form, contain some amount of boron [4,5]. The only exception, probably, is the cast Ti48Al2Cr2Nb, which was due to the fact that it was developed in parallel with the boron-containing alloys represented by the exothermically dispersive (XD) Ti45Al2Mn2Nb1B and Ti47Al2Mn2Nb1B (both contain ~0.8vol% TiB_2). The XD TiAl alloys descended from TiAl-TiB_2 composites containing 7-15vol% TiB_2 and after composition optimisation 1% (atomic percentage thereafter unless stated otherwise) boron was found to be enough to give rise to fine lamellar colonies with sizes between 50-150μm in as-cast Ti(45-47)2Mn2Cr1B alloys [4,6,7]. Since then, boron has been firmly related to 'grain refinement' in cast TiAl alloys. Indeed, boron rarely (rarely but never) failed in refining as-cast microstructures of TiAl alloys with various compositions [8]. In addition to the obvious grain refinement in cast alloys the effects of boron addition in other respects of physical metallurgy and mechanical metallurgy, such as solidification, phase transformation kinetics, fracture behaviour etc., have been gradually realised and studied over the years, and a fairly large body of knowledge about boron in TiAl alloys has been accumulated. The aim of this review is to collect boron-related information from TiAl literature and to organise them into themes, for the convenience of researchers in the future as boron having been an alloying element of convenience in TiAl alloys in the past.

2 Grain refinements in cast TiAl alloys

2.1 The observation of grain refinement

Grain refinement has been the primary role of boron in cast TiAl alloys since boron was first introduced into TiAl systems. Simplicity and practicality of this technique, to a large extent, bestowed vitality on it. It works well with many boron sources, such as titanium borides, aluminium borides, and even tantalum borides, tungsten borides and lanthanum hexaboride, where composition permitting, so long as the molten pool is maintained long enough to fully dissolve borides and to homogenise boron distribution in the liquid [9-11]. Grain refinement occurs during production casting process and ingot making process. It was even observed in gas atomised Ti45Al2Mn2Nb1B powder particles which were subject to very fast cooling during solidification [12]. Figure 1 shows the macrostructures of Ti48Al2Cr2Nb(1B) 25kg ingots produced via cold hearth

plasma arc melting. In contrast to the coarse columnar structure in Ti48Al2Cr2Nb the fine lamellar colonies in Ti48Al2Cr2Nb1B are equiaxed with an average size of 200μm.

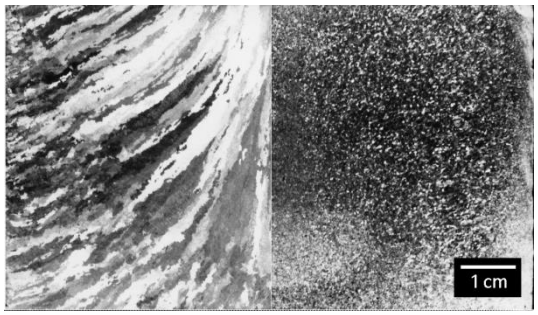

Fig. 1 Macrostructures of (left) Ti48Al2Cr2Nb and (right) Ti48Al2Cr2Nb1B ingots.

Based on the experimental results of a few Ti47Al2Mn-X (X=V, Cr, Nb at 1-2%) the relationship between boron concentration and grain size was established as in a form of inverse variation curve as shown in Fig.2 [13]. It can be seen from the curve that significant grain refinement only occurred when boron concentration reached a certain level, i.e. the critical boron concentration. No grain refinement with boron below it. This phenomenon was referred to as the 'Switch on/off' effect. No marked further grain size reduction with increasing boron concentration. For Ti47Al2Mn2Nb1B (the best performing alloy in the lot, with boron above the critical boron concentration) the grain size was about 100μm. In low alloying TiAl alloys with peritectic reaction the critical boron concentration is about 0.5-0.8% [9].

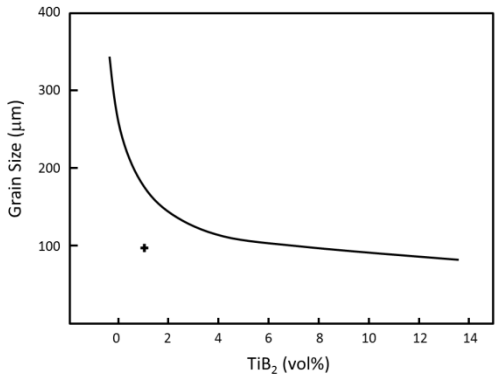

Fig.2 Relationship between boron concentration and grain size in cast Ti47Al2MnX alloys [13]. The cross (+) was from Ti47Al2Mn2Nb1B.

Grain refinement has been observed in a few tens TiAl alloys with about 1%B in various forms, such as investment cast materials and ingots weighing from 20g to 50kg. By summarising some results it was found in 2001 that the Al concentration and some refractory elements like W and Ta have a strong influence on the resulting grain size (lamellar colony size in another term), i.e. increasing their concentration leading to large grain size [8]. Limited by the knowledge of solidification process in those alloys the phenomena were not satisfactorily explained at that time. Now, it is fairly clear that such an influence is highly likely to be asserted through changing the solid/liquid phase ratio of the peritectic reaction.

Beta-solidifying TiAl alloys have attracted increasing attention since 2005 and the recently developed beta-gamma and TNM alloys contains about 0.1% boron [14,15]. Alloys of the two families were designed as wrought alloys but fine starting microstructures are essential for thermomechanical processing. Hence, 0.1% B was added to produce fine grains after solidification. In contrast to the critical boron concentration in early TiAl alloys the required boron concentration for grain refinement in β-solidifying alloys is very low. Our data shows that 0.1%B is enough in binary Ti44Al let alone heavily alloyed β-solidifying alloys. In Ti44Al8Nb 0.075% B gave rise to grain refinement whilst 0.05%B led to coarse Widmanstätten α grains. Figure 3 shows the as-cast microstructures of the three alloys in form of 20g ingots. Boron addition beyond 0.1% did not show marked further reduction in alpha grain size, but changes in other aspects of which phase transformation texture is one of them.

(a)

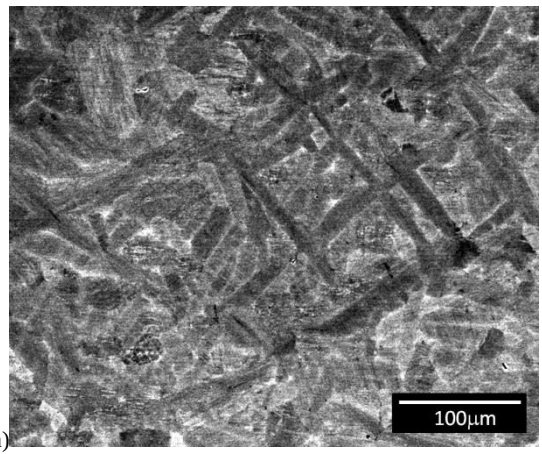

(b)

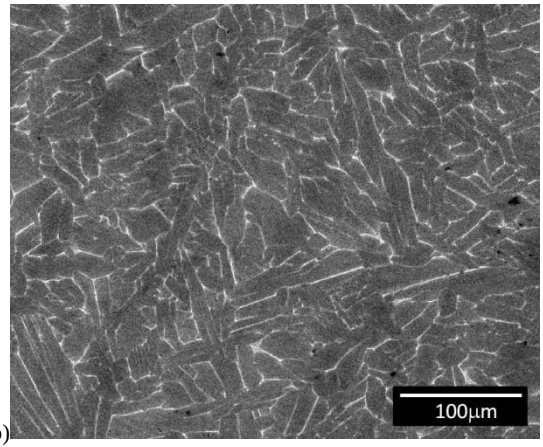

(c)

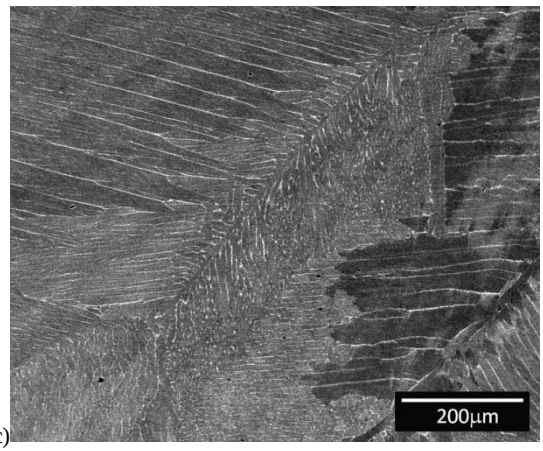

Fig.3 SEM BSE images showing as-cast microstructures of 20g ingots: (a) Ti44Al0.1B, (b) Ti44Al8Nb0.075B and (c) Ti44Al8Nb0.05B.

The refined microstructures have two properties: grain/lamellar colony size and lamellar orientation distribution. The first is a commonplace but the second has not been paid enough attention in microstructural characterisation. The term of phase transformation texture means that many α grains descended from the same β dendrite and some of them may have preferred orientations since the Burgers orientation relationship between α and β phase may be obeyed during transformation. Thus, the orientation distribution of lamellar colonies could be very different in grain refined TiAl alloys even though the grain size could be very similar. A simple method of measuring the texture was developed by the author in 2009. It is as such that the angle between the lamellar interface trace of each lamellar colony in a micrograph with respect to one graph edge is measured and the number frequency is plotted against the angle [16]. Figure 4 shows the example of lamellar orientation distribution in cast Ti44Al8Nb with 0.1 and 1%B. The lamellar orientation distribution of Ti44Al8Nb0.1B is significantly different to that of Ti44Al8Nb1B, being concentrated at a few angles.

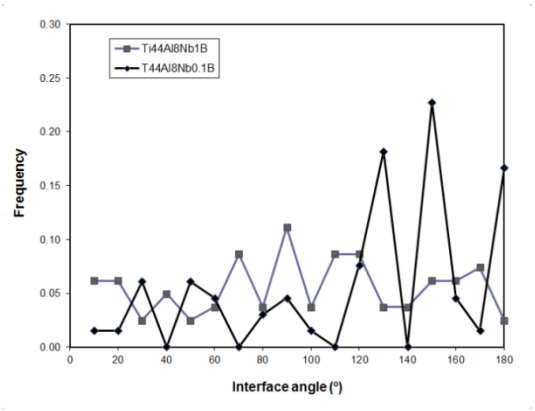

Fig. 4 Lamellar orientation distribution of cast Ti44Al8Nb0.1B (1kg ingot) and Ti44Al8Nb1B (50kg). Average grain size is 70μm to 75μm.

2.2 Grain refinement mechanisms

Investigation into grain refinement mechanism started probably at the same time of introducing boron into TiAl alloys and has lasted to date. Grain refinement in TiAl-B systems, at its very essence, is based on boron's unique partitioning behaviour between the solid phases and the liquid phase. Its solubility in α_2-Ti_3Al and γ-TiAl phases at room temperature was found to be <0.003 and only 0.011at% respectively [17]. There is no data for elevated temperatures and no data for β/B2 phase. In light of the observation of thin curvy boride formed in the interdendritic liquid of some Ti(43-45)Al(5-8)Nb alloys with >0.1% boron and the absence of such boride precipitates in the alloys with only 0.1% boron the boron solubility in the β phase at the solidification temperatures (>1500°C in Ti44Al8Nb1B) is estimated as close to 0.1% [18-20]. In an attempt to reassess the Ti-Al-B system, boron solubility in the α, β and γ phases at high temperatures was calculated by Witusiewicz *et al*., giving so far the best estimation [21].

A direct result of the low boron solubility is the high partition of boron to the liquid. As a consequence, a boron-rich layer in the liquid is formed next to the solidification fronts as soon as solidification starts. Such a boron-rich layer forms a constitutional undercooled zone, which could have an effect of preventing solid phase growth in the liquid. Limited β grain growth in as-cast Ti and Ti-X binary alloys was reported by Bermingham *et al* in 2008 where it was partially attributed to the compositional undercooled zone effect [22]. This concept can be further traced back to Al and alloys [23]. Limited β dendrite growth by B addition has been observed in Ti45Al2Mn2Nb1B but not in all TiAl-based alloys [24]. Thus, great caution has to be exercised when applying this theory to complex TiAl alloy systems.

2.2.1 Pre-2007 era

The grain refinement studies over the years can be separated into two eras with a turn at 2007. In the pre-2007 era there was almost no dedicated effort to investigate grain refinement mechanism and the proposed mechanisms were often the by-products from general research activities. The proposed mechanisms were very much based on reasoning from fragmentary observations. In those early proposed mechanisms the applicable ranges were not defined and most of them have not been purposely verified by designated experiments. A few early grain refinement mechanisms were summarised by Cheng in 2000 [25]. In 1990 Larsen et al proposed the earliest mechanism based on their work on the XD TiAl alloys containing 0.1-4.6 vol% TiB_2 in which the grain refinement was attributed to the inoculation by titanium boride added to the alloy but not fully dissolved during melting [4]. This mechanism was further studied by Gosslar *et al.* in 2009 through calculating the efficacy of nucleating β or α solid in the liquid by TiB_2 with different pairing crystal planes. It was demonstrated that the pre-existing boride particles were capable of inoculating β solid in the melt [26,27]. However, most TiAl-B alloys after the early XD alloys/composites contain up to only 1% boron, rendering the alloys at the hypoeutectic side where pre-existing boride particles is not possible when fully melted. Thus, the mechanisms proposed after that were related to precipitation of borides after a metallic primary phase during solidification.

Inkson *et al.* proposed a mechanism of simultaneous nucleation in 1993. In this mechanism primary boride and the beta phase within the melt to form boride precipitates interleaved with beta phase and the borides acted as nucleation sites for the metallic phase in a TiAl alloy doped with Fe and V [28]. Indeed, in many TiAl-B alloys ribbon-like TiB_2 or TiB precipitates were found to have interlaced structure with the β/B2 phase [9,29]. Such a simultaneous nucleation, which is somewhat eutectic reaction-like, has not been supported by simulated phase diagrams.

Shortly after Inkson's work a mechanism of fragmented dendrite arms was proposed by Godfrey in 1996 [30]. It was suggested that the boron addition weakened the roots of dendritic arms during solidification (probably by the growth limiting effect of boron segregated into the liquid) and the dendritic arms were broken off from the dendrites by convection into the liquid as new grains/dendrites.

Cheng also produced a mechanism based on constitutional undercooling theory [25]. Owing to the great partition of boron from the solid into the liquid at the solidification front, when alloys contain enough boron, the constitutional undercooling could reach an extent so high that homogeneous nucleation of solid phase could occur, which increases nucleation density. The increased nucleation density is the cause of grain refinement and the newly nucleated grains are independent from the early solid in orientation. This mechanism explained fine grains, random orientation and the critical boron concentration.

What is common in the three mechanisms but not mentioned explicitly is that it is the β phase, the primary solidifying phase, is refined since all the studied alloys solidify through the β phase or through L+ β → α peritectic reaction. However, what we mean by grain size is the size of lamellar colonies which is inherited from the prior α grains in those alloys. A small β grain size will not always lead to a small α grain size and the latter is very much related to the way in which the β → α solid phase transformation occurs and the extent of peritectic reaction. That is something all the previous mechanisms failed to address.

2.2.2 Solidification path-related era

Since 2007 the grain refinement study has been linked to alloy solidification path. TiAl alloys can solidify via L → β, L+ β → α, L → α, L+ α → γ and L → γ different paths with increase Al concentration [31]. To date grain refinement study has covered alloys up to α solidification, leaving the last two almost untouched.

2.2.2.1 β solidification

In Ti-Al binary alloys with Al concentration lower than 44.8% or other heavily β stabilised alloys solidification is completed fully through the β phase and a β → α solid phase transformation follows thereafter. Imayev *et al.* showed in 2007 that boron concentration as low as 0.1% can refine the lamellar colony size in β-solidifying TiAl alloys through titanium boride precipitates' inoculation of α phase during β → α solid phase transformation [32]. It is common knowledge that the β → α solid phase transformation occurs in a Widmanstätten manner under normal cooling conditions. Usually, the Burgers orientation relationship, $(0001)_\alpha//\{110\}_\beta$ and $<11\,\overline{2}\,0>_\alpha//<111>_\beta$, is obeyed between α and β [33]. In theory there could be as many as 12 α-variants. However the nucleation of a hcp phase in a bcc matrix is difficult since the coherency at the interfaces is very low. A large energy barrier needs to be overcome in order to nucleate the hcp phase. In reality only a few α-variants have the chance to nucleate, with the help from the β grain boundaries, and grow and often the α laths with the same orientation band together to form a large α grain, as shown in Fig.3c. The situation is entirely different when boride precipitates are present before β → α solid phase transformation starting. Boride precipitates can act as inoculants to help *a* phase nucleate. This idea was first presented by Imayev *et al.* and was later by many other researchers [18,19,34]. Recently, Kartavykh *et al.* reported

direct observation of α_2-Ti_3Al phase nucleating at and growing off boride precipitates in an alloy with 0.4% B [35]. With boride inoculation most, if not all, of α-variants can nucleate. Figure 5 shows the α_2-variants in an as-cast Ti44Al8Nb0.1B. The (0001) poles of α_2-Ti_3Al obtained using electron backscatter diffraction (EBSD) analysis is in Fig. 5a and the circled 6 clusters are corresponding to the {110} positions of the parent β phase. Figure 5b shows orientation map of the α_2-Ti_3Al grains, in which individual variants are identified. The variants with the same number have their basal planes on the same $\{110\}_\beta$ plane and the apostrophe of the number denotes the second variant on the same $\{110\}_\beta$ plane (two a variants on each $\{110\}_\beta$ plane). It can be seen that all 12 α-variants are present, in stark contrast to the Widmanstätten type microstructure in Fig.3c. With more α-variants the resulting α grains should be smaller.

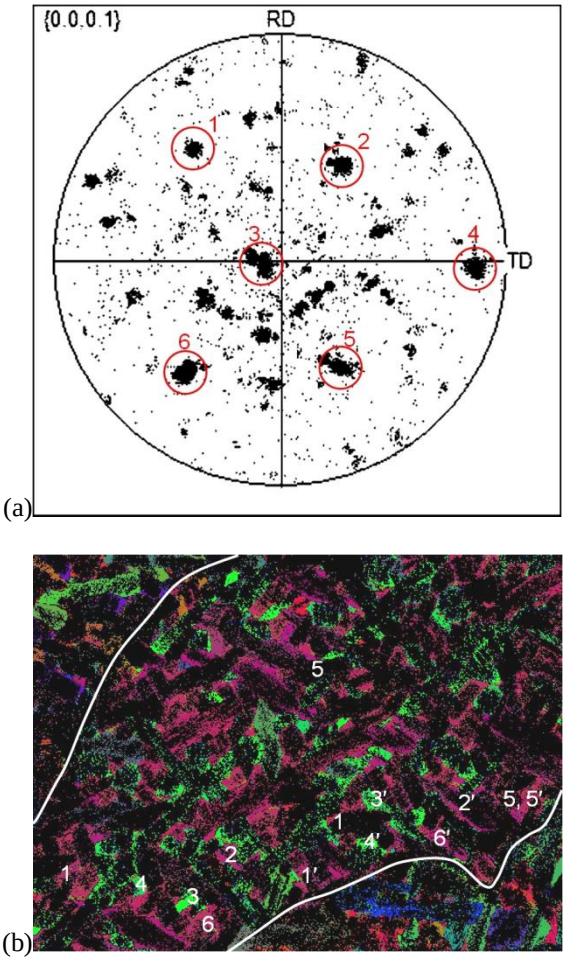

Fig. 5 EBSD analysis on α_2-variants in as-cast Ti44Al8Nb0.1B 20g ingot. (a) (0001) pole figure of α_2-variants and (b) orientation map with α_2-variants in the middle β grain labelled.

Now that the grain size in β-solidifying TiAl alloys can be refined by addition of 0.1% B there is still a critical boron concentration since no grain refinement in Ti44Al8Nb0.05B (Fig. 3c). Detailed microstructural examination on the as-cast Ti44Al8Nb0.05B revealed fine boride precipitates. The fine rod-like particles with bright contrast in Fig. 6 are TiB. They are not randomly distributed throughout the alloy matrix but located at certain loci shown as bright ridges. The bright ridges were formed during β → α phase transformation at a late stage when heavy β stabilising element Nb was expelled from the α laths into the remaining β, contributing to the bright contrast in the BSE image. The preference of TiB precipitates to the white ridges suggests that they would have formed after the start of β → α phase transformation. The α laths were already there when the boride were formed and the boride precipitates, thus, could not apply any inoculation effect on the existing α phase. Therefore, it is quite clear that the critical boron concentration in β-solidifying TiAl alloys is the boron concentration required to form boride precipitates BEFORE β → α phase transformation starts.

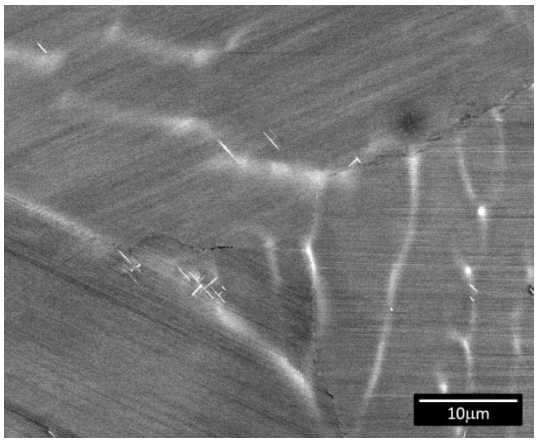

Fig. 6 SEM BSE image showing fine TiB precipitates in as-cast Ti44Al8Nb0.05B 20g ingot without grain refinement.

Similar to the trend shown in Fig.2 further increasing boron concentration beyond the critical concentration does not lead to significant further reduction in lamellar colony size, as manifested by the average lamellar colony size of 70 to 75μm mentioned in the caption of Fig.4 from Ti44Al8Nb0.1 1kg ingot and Ti44Al8Nb1B 50kg ingot [36]. However, increasing boron beyond the critical concentration changes the way in which boride forms and its morphology. Figure 7 shows the as-cast microstructures of Ti44Al8Nb with 0.1, 0.3 and 1B. The inserts shows typical boride morphology in those alloys. A slight reduction in the length and width of α laths can be seen with increasing boron from 0.1 to 0.3 but such changes will not always translate into lamellar colony size since each α grain, the size of which underpins lamellar colony size, is often composed of many parallel α laths. Marked difference in the morphology of boride precipitates can be seen in

alloys with different boron concentrations. In the 0.1B alloy boride precipitates are thin and straight, not more than 30μm in length. This is the typical feature of solid precipitation, i.e. the boride precipitates formed within the β matrix. In the 0.3B alloy some thin, curvy boride precipitates can be frequently found at the interdendritic areas and in some cases a chain of them can be as long as 100μm, as shown in the insert of Fig.7b. Such boride precipitates were also found in some TiAl alloys with 0.2B and they were formed in the liquid between dendritic arms [18]. In Ti44Al8Nb1B boride precipitates have different morphologies, some being thick and long, some being thick and short and some being blocky. The different morphology of boride precipitates in the same alloy can be attributed to the different solidification stages in which they were formed. Those forming at the very beginning of solidification had enough time and space to grow into long planks without being disrupted and those precipitating at the end of solidification had no time and space to grow. What is in common for the curvy boride precipitates in the 0.3B alloy and those in the 1B alloy is that they were formed from liquid.

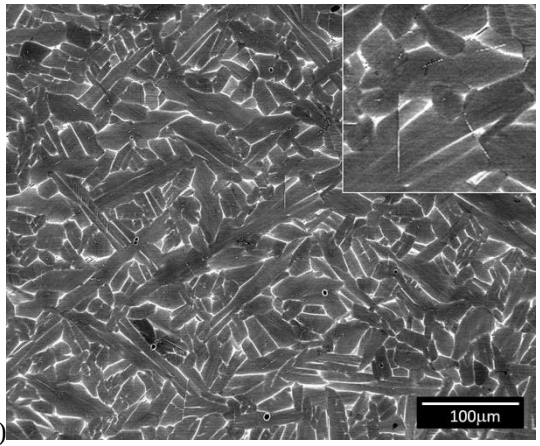

(a)

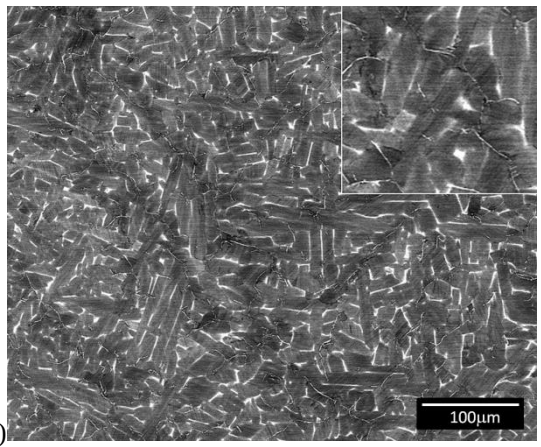

(b)

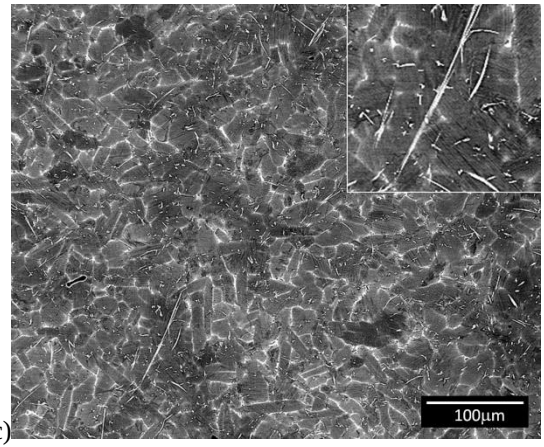

(c)

Fig. 7 SEM BSE images showing as cast microstructures of 20g ingots of Ti44Al8B with: (a) 0.1B, (b) 0.3B and (c) 1B.

One important difference between boride precipitates forming from liquid and from solid lies in their orientation relationship with the solid phase they are embedded in. Generally there are orientation relationships between the thin straight boride precipitates and the surrounding solid phases. Some of them have been identified. Between α_2 and TiB (B_f) a specific orientation relationship was observed in Ti44Al8Nb0.1B which is $[10\bar{1}2]_{\alpha2}$ // $[001]_{Bf}$ and $(1\bar{2}10)_{\alpha2}$ // $(010)_{Bf}$ [19]. It is not clear which of the two, this particular TiB precipitate from which the above OR was measured and the α_2 grain the TiB precipitate was in, formed first during solidification and there is no evidence that this α_2 grain was inoculated by this precipitates. It is possible that the TiB precipitate had an OR with the β grain in which it was formed and the α grain surrounding the TiB was a Burger α variant, thus inheriting the OR between TiB and β. By incorporating the Burgers OR, $(0001)_\alpha$//$\{110\}_\beta$ and $<11\bar{2}0>_\alpha$//$<111>_\beta$, into the measured one between TiB (B_f) and α_2 it is verified that in the β-α_2-TiB system their orientation relationships are interchangeable.

The orientation between γ and TiB (B27) was identified in an as-forged Ti45Al8Nb0.2W0.2B0.02Y as $[010]_{B27}$//$<110>_\gamma$ and $(100)_{B27}$//$\{112\}_\gamma$ [37]. It is highly likely that the studied TiB particle was present before forging considering its fairly large size (0.7μmx2μm of a cross section). What is not sure is whether the γ grain having the reported OR with the B27 particle was a result of dynamic recrystallisation. If it is the case the γ grain nucleated on the B27 particle during recrystallisation and establishing the OR between themselves. Or it inherited an OR with the B27 particle from its parent α phase. Nonetheless, after substituting the Blackburn orientation relationship between α_2 and γ, $(0001)_{\alpha2}$ // $\{111\}_\gamma$ and $<1\bar{2}10>_{\alpha2}$ // $<110>\gamma$, the OR between α_2 and B27 is deduced as $<1\bar{2}10>_{\alpha2}$ // $[010]_{B27}$ and $(0001)_{\alpha2}$ // $(001)_{B27}$.

This OR has been found in Ti44Al8Nb1B between B27 boride and the α_2 grain inoculated by it [34].

For most of the boride particles precipitated from liquid there is no orientation relationship between them and the matrix. Only for the boride particles having inoculated α grains there are orientation relationships between them and the α grains. Bearing in mind that each α grain needs only one boride particle to inoculate it and considering the large number of boride precipitates and the small number of lamellar colonies the chance of finding orientation relationship between boride and lamellar colony is very small in TiAl alloys with boron concentration well above the critical concentration.

Despite the lack of further grain refinement by excessive boron significant change in microtexture (which is such termed owing to fact that the scale of texture is limited to the prior β grain size) can be brought in as shown in Fig.4. In the alloy with 0.1B most of the boride precipitates had certain orientation relationship with the β phase and inoculated α grains obeying the Burgers OR with the β phase. Such α grains are referred to as the 'Burgers α' and the others as the 'non-Burgers α'. The Burgers α can be regarded as textured since many of them have their basal plane and *a*-axis parallel to the others'. Hecht *et al* first noticed that in their alloys containing 0.2B there are two types of α grains; one with Burgers OR and one without [18]. Also, the non-Burgers α grains were found mainly in the interdendritic areas where thin curvy boride precipitates were present. Those boride precipitates were formed from the liquid and held no orientation relationship with β dendrites. It is those boride precipitates that inoculated the non-Burgers α grains in the interdendritic areas. Yang *et al.* furthered the understanding of relationship between boron concentration and microtexture by quantitatively analysing the microstructures shown in Fig. 7 using EBSD [19]. It was found that the extent of microtexture, in terms of the portion of Burgers α grains, was reduced from around 85% with 0.1B to only about 20% with 1B. It can be seen that the extent of microtexture in the as-cast 1B alloys is equivalent to that in the forged and heat treated alloys comparing Fig. 4 with that in [16].

Before finishing this section it is worth to reiterate a fact that the earliest recorded the observation of grain refinement by low dose of boron addition in β-solidifying TiAl alloys was published in 2005 by Wang *et al.*, about two years before Imayev's publication [38,32]. They demonstrated fine acicular microstructures, which developed into fine lamellar colonies about 50μm in average after heat treatment, in an as-cast Ti44Al6Cr2Nb0.5W0.15B. However, they did not realise the success as they are quoted as saying that 'The low amount of B (0.15%) was added to slow down grain growth during heat treatment. It is not for grain refinement during solidification because a large amount of B (generally >0.5%) is needed for refining the cast microstructure.' This figure (>0.5%) was quoted from [9] and was not for β-solidifying alloys, which was not known then but known now.

2.2.2.2 $L + \beta \rightarrow \alpha$ peritectic reaction

Most of the TiAl-B alloys studied for grain refinement have solidification paths through the $L + \beta \rightarrow \alpha$ peritectic reaction before the β-solidifying alloys coming to fashion. In binary Ti-Al system it covers the alloys with Al ranging from 44.8 to 49.4% [31]. Alloying will change this range and one example was given by Chen *et al.* regarding Nb addition [39]. Alloys in this category solidify through β phase first. At the peritectic reaction temperature the remaining liquid reacts with β solid to form peritectic α at the liquid/β interfaces. The peritectic α nucleates on the surface of the β solid and grows into both liquid and the β solid. Quite often the peritectic α nucleated at one side can grow across the liquid region to consume the β solid at the other side which may not belong to the same β crystal. In view of the difficulty in nucleation a small number of peritectic α grains can grow into very large size between/along β dendrites, forming coarse columnar structures. With increasing Al the portion of remaining liquid for peritectic reaction is lager and the resulting peritectic α grains will be coarser under the same solidification conditions. Therefore, the peritectic α grains have to be refined to have fine-grained microstructures.

Figure 8 shows a fine microstructure in as-cast Ti45Al2Mn2Ta1B. Ta was added to increase the contrast of the BSE images by its strong segregation tendency to reveal the details of the microstructures. In this micrograph there is no trace of columnar α grains but nearly equiaxed lamellar colonies with their boundaries delineated. The lamellar colony size is very heterogeneous and the large lamellar colonies are centred at interdendritic areas, covering different β dendrites surrounding them. At some places one β dendrite was consumed by two peritectic α grains from opposite sides. The small colonies are mainly in the stems of dendrites. Such phenomena were also observed even in some other alloys, such as Ti44Al5Nb0.85W0.85B, which should be β-solidifying but deviated to peritectic reaction at the end of solidification due to strong segregation of Nb and W [40]. Those observations manifest the importance of controlling peritectic α grain size in the process of grain refinement.

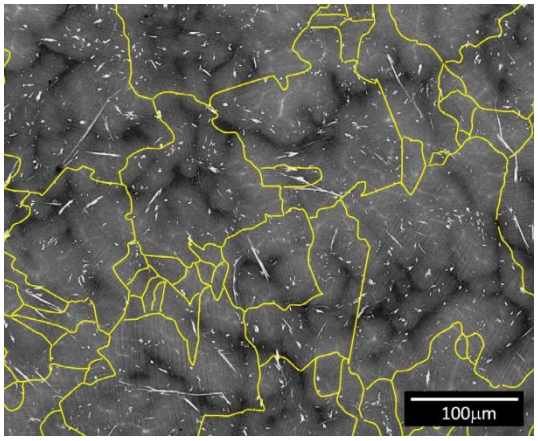

Fig.8 SEM BES image of as-cast Ti45Al2Mn2Ta1B, showing dendrites and lamellar colonies.

Recent work on grain refinement mechanisms of alloys with L + β → α peritectic reaction solidification paths shows new progress. Some Ti45Al2Mn2Nb1B Bridgman specimens were prepared and detailed microstructure and EBSD analysis were carried out on the solidification zone [24]. Figure 9 shows the microstructure and α_2 EBSD orientation map of the solidification zone in Ti45Al2Mn2Nb1B. The black areas in the orientation map is γ-TiAl phase formed during quenching at the final stage of Bridgman sample preparation. Two key facts were found in Fig.9. Firstly, most of the α_2 grains have no Burgers orientation relationship with β dendrites. Secondly, some separated α_2 grains in a same interdendritic area (those labelled with the same number and having the same colour in the orientation map) have the same orientation. They are actually of a same grain separated by the γ phase wrapped in the middle. It seems that once a peritectic α grain was nucleated it could soon grew along the solid/liquid interfaces regardless of the orientation of the surrounding β dendrites and grew into them. One section of a β dendrite in Fig. 9 (numbered 9, 20-24) was consumed by different peritectic α from both sides.

(a)

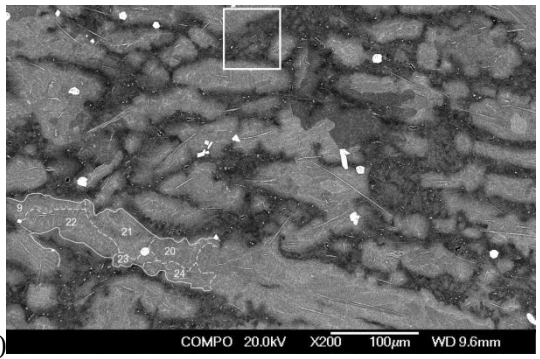

(b)

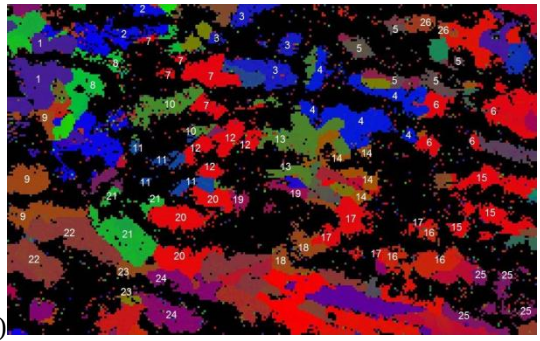

Fig. 9 Solidification zone in a Ti45Al2Mn2Nb1B Bridgman specimen. (a) SEM BSE image and (b) EBSD orientation map of α_2 phase.

The nucleation of peritectic α was found to be through the exiting boride precipitates in the interdendritic areas. One example is given in Fig.10 where the orientation relationship between boride precipitates and α_2 grains is shown. The pole figures were taken from the rectangle area in Fig.9a covering α_2 grains No.3 and boride precipitates within the selected area. In spite of many boride precipitates in this area only one was found to have an orientation relationship of $<1\ \bar{2}\ 10>_{\alpha 2}$ // $[010]_{B27}$ and $(0001)_{\alpha 2}$ // $(001)_{B27}$ with the α_2 grains, which should be their inoculant. Thus, it is fairly confident to say that the grain refinement mechanism in TiAl-B alloys with peritectic reaction solidification paths is as such that the existing boride precipitates inoculate peritectic α in the interdendritic areas and the peritectic α grow into both β dendrites and liquid. The peritectic α acquires orientation from the inoculating boride precipitates. The critical boron concentration is that forming enough boride precipitates before peritectic reaction starts. There are still some α_2 grains having Burgers orientation relationship with β dendrites but most of them were found at the middle of the stems of β dendrites and away from the interdendritic areas as observed in Ti45Al2Mn2Nb1B powder particles [12].

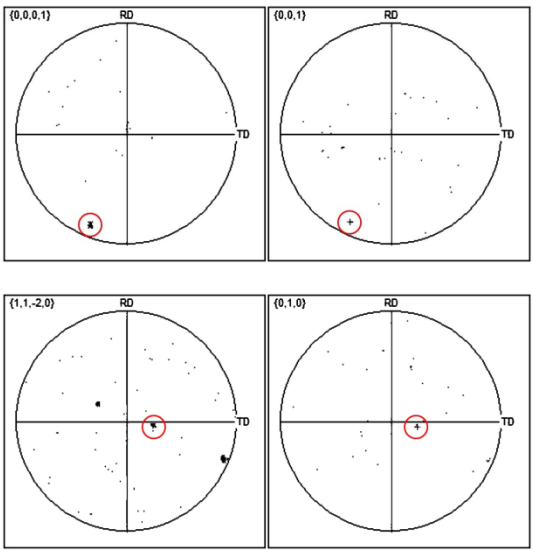

Fig. 10 Pole figures from the selected area in 9a showing orientation relationship between a TiB (B27) precipitate and α_2 grains No. 3.

2.2.2.3 α-solidification and beyond

Alpha solidification occurs in binary TiAl alloys with aluminium concentration in the range of 49.4 and 51% under equilibrium (or nearly) conditions [31]. Practically solidification of such alloys would inevitably shift to L + α → γ at a later stage owing to segregation. Data of grain refinement in alloys of this category is rare. One case was reported in 2001 where the concerned alloy was Ti50Al2Cr2Nb1B [8]. The α phase was believed to be the primary phase of solidification based on the observation of lamellar interfaces orientation with respect to the parent dendrites' growth direction. The as-cast microstructure was lamellar with an average colony size of about 280μm. There has not been enough work on those alloys to date to establish grain refinement mechanism but the effort is still continued.

TiAl-B systems with higher Al concentration at 52% were reported. However, only the morphology of TiB_2 was investigated and no information on grain refinement was disclosed [41].

3 Boron effect on solidification behaviour

In most of the studied TiAl alloys the primary solidification phase is the β phase no matter what follows thereafter. The width of L + β phase field varies with Al concentration and other alloying elements. According to Okamoto's Ti-Al phase diagram the maximum L + β phase field is about 50°C in Ti-44.8Al [31]. Increasing Al concentration reduces the L + β phase field, e.g. being ~30°C at 46%Al. Adding 8% Nb to Ti-46Al not only increases the liquidus by ~50°C but also enlarges the L + β phase field to ~85°C according to Witusiewicz *et al*. [42]. In cast alloys the width of the L + β phase field, also referred to as the 'freezing range', affects the fluidity of the molten metals [43]. In general, shorter freezing range leads to better fluidity which is essential to fulfil the moulds during casting. Mould filling is of the upmost importance in casting. This issue was not addressed in the development of cast TiAl alloys, at least not openly. Only until the ISGTA 2014 did Zhang praised the better castability of a TiAl alloy with 48% Al and attribute it to the shorter freezing range from high Al concentration [44].

Boron addition to TiAl alloys may reduce the freezing range of solidification. It has been known in private for years that some alloys containing boron at 1% have better castability compared to their boron-free counterparts [45]. The reason may lie in the shorter freezing range of boron-bearing alloys. The work on the solidification of Ti45Al2Mn2Nb(1B) showed that the solidification zone of Bridgman samples was nearly halved in length in the boron-bearing alloy and the β dendrites were thinner and shorter under the same solidification conditions [24]. Such changes can only be induced by boron addition. The experiment results were supported by studies on phase diagrams by Witusiewicz *et al*. in which it was clearly shown that in Ti-47.4Al the L + β phase field width was reduced to zero from about 30°C by 1.1% of boron [21]. The schematic phase diagram of Ti47.4Al-B is shown in Fig.11. The shorter freezing range coupled with finer β dendrites, likely resulted from the growth limiting effect of boron segregating to the solidification front, could lead to the better castability. Recently results from designated fluidity tests showed that some boron-bearing TiAl alloys had longer maximum fluidity length than the boron-free base-alloys, though this effect is not universal [46]. Nonetheless, this area is worth further exploring and understanding in order to develop designated cast TiAl alloys.

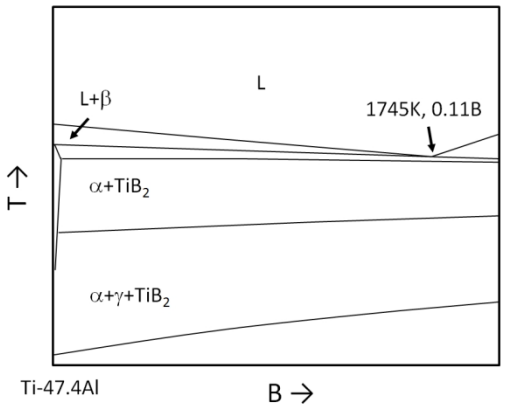

Fig. 11 Phase diagram showing boron effect on the L+b phase field in Ti-47.4Al [21].

4 Boron effect on fracture behaviour

As mentioned earlier that adding boron rarely failed to refine microstructures in cast TiAl alloys. In contrary, the benefits of fine microstructures in cast TiAl alloys are not always transferred to properties. Taking room temperature tensile ductility as an example, the improvement was evident in some alloys, but not in others. Tensile ductility in cast Ti48Al2Cr2Nb with coarse columnar structure (lamellar colony size of ~1mm) shown in Fig.1 is hardly more than 0.2% at room temperature whist that in the grain refined Ti48Al2Cr1Nb1B ingot can reach 1% [47]. It seems that processing also can affect whether small grain size can lead to good tensile ductility. A study on investment cast

Ti46Al8Nb1B showed that the tensile ductility varied from 0.8% to 0.2% when the cast bar diameter was increased from 15mm to 30mm [48]. Microstructural characterisation revealed no significant change in lamellar colony size. However the change in cooling conditions of solidification due to change in cast bar size led to marked change in boride precipitate size. The ductility-grain size relationship in TiAl alloys was established in the early 1990s [3]. It is as such that reducing grain size increases ductility monotonically and the curve has an inverse function shape similar to that of grain size versus boron concentration in Fig.2. The presence of titanium boride precipitates has changed this relationship and they are believed to effect via influencing crack nucleation and growth behaviour.

4.1 Titanium borides in TiAl alloys

It is helpful to briefly summarise the knowledge on titanium borides in TiAl alloys gained in the past. There are four types of titanium borides found in TiAl alloys: TiB_2, Ti_3B_4, TiB (B27), and TiB (B_f) in the order of boron concentration. Their crystalline information was summarised by De Graef *et al* in 1992 and some basic information is listed in Table 1 [49]. Those borides were often found co-existing and therefore there are orientation relationships between them. They are $[010]_{B27}$ // $[001]_{Bf}$ and $(100)_{B27}$ // $(110)_{Bf}$, $[100]_{Bf}$ // $[100]_{D7b}$ and $(010)_{Bf}$ // $(010)_{D7b}$, $[100]_{Bf}$ //$[0001]_{C32}$ and $(010)_{Bf}$ // $\{10\bar{1}0\}_{C32}$ [49]. Some of the ORs were reported again later by Kitkamthorn *et al.* [29].

Table 1 Crystal structure and lattice parameters in titanium borides observed in TiAl alloys

Structure	Space group	Lattice parameter (nm)
TiB_2 C32	P6/mmm (no.191)	a = 0.303
		c = 0.323
Ti_3B_4 $D7_b$	Immm (no. 71)	a = 0.326
		b = 1.373
		a = 0.304
TiB B27	Pnma (no.62)	a = 0.611
		b = 0.305
		a = 0.456
TiB B_f	Cmcm (no.63)	a = 0.323
		b = 0.856
		a = 0.305

What concerns casting of TiAl alloys is the growth direction of titanium borides in the molten metals and it is the anisotropic growth that shapes the morphology of boride precipitates. A systematic study, probably the only one, on TiB_2 morphology in TiAl alloys was published in 1991 [41]. It detailed the anisotropic response of crystal growth of TiB_2 to the change in undercooling/cooling rate during solidification. The growth rate along the *c*-axis and lateral directions vary differently with boron concentration and cooling conditions, leading to different aspect ratio of TiB_2 precipitates and giving rise to different morphologies. Under the casting conditions of the Ti48Al2Cr2Nb1B ingot shown in Fig. 1 the TiB_2 precipitates take a plate-like morphology with an aspect ratio of about 10-20. The length is along the *c*-axis, usually not more than 50μm [8]. Under certain conditions, such as low boron concentration or fast cooling, TiB_2 precipitates can adopt a flake-like morphology with a thickness normally less than 0.5μm and a very large aspect ratio up to 100 [41]. Its dominant surfaces are $\{1\bar{2}10\}$, indicating fast growth along [0001] and $<10\bar{1}0>$. The growth rate order is $[0001] \geq <10\bar{1}0> >> <1\bar{2}10>$, judged from the TEM image and the selected area diffraction (SAD) pattern of the analysed TiB_2 flake. The flake-like TiB_2 precipitates are formed in the molten metal and constrained by the primary phase during growth and thus have curvy shapes. They are shown on sample surfaces as thin curvy lines owing to intersection effect and sometimes referred to as 'curvy borides'.

The growth of titanium monoborides (TiB) appears more anisotropic than TiB_2. There is no published systematic study on TiB morphology although work has been underway for some times. From patchy information scattered in the literature it is known that TiB also has different morphologies. The two most often observed of B27 TiB are plank-like and flake-like (curvy) morphologies. The broad surface of plank-like TiB (B27), formed during solidification under slow and medium cooling conditions, is $(100)_{B27}$ which means the slowest growth direction is $[100]_{B27}$ [8,37]. The longest dimension is along the $[010]_{B27}$ [35]. The aspect ratio of *a*:*b*:*c* can be 1:20-100:3-10. Also TiB (B27) precipitates can grow into very large size [8,48]. The longest observed by the author is about 200μm in length, ~1μm thick and ~10μm wide.

The information on morphology and size of TiB (B_f) precipitates are very limited. Compared to TiB (B27) the B_f structured TiB is less common. Recently Kartavykh *et al.* summarised the type of boride in high Nb containing TiAl alloys and found the prevailing form was B27 [50]. TiB (B_f) was found in a Ti44Al8Nb1B and Ti44Al4Nb4Zr1B 1kg button ingots [25,29]. Also it was in a Ti44Al8Nb0.1B 20g finger ingot [19]. All the occasions were related to fast cooling during solidification. There has been no report on observation of long and thick TiB (B_f) precipitates. From TEM analysis it was found that the longest direction of TiB (B_f) precipitates is $[100]_{Bf}$ with the shortest direction of $[010]_{Bf}$ [19,29].

4.2 Cracking at boride/matrix interfaces

Titanium borides are hard and have Young's modulus of 450-550GPa whist it is only 150-180GPa for the matrix. The large difference in modulus means that the plastic deformation (slip and twinning) will occur in the matrix and

stops at the boride/matrix interfaces, causing severe stress concentration. The intense stress concentration will inevitably lead to cracking at the interfaces via debonding or other means. Figure 12a shows the fracture surface of tensile tested Ti44Al8Nb1B in the form of ϕ30mm investment cast bar. The long facets are the failed interfaces of TiB planks most of which are about 100μm long, equivalent to average lamellar colony size. The measured ductility is a mere 0.2%. Figure 12b shows a facet on the fracture surface of cast Ti45Al2Mn4Nb1B and the facet is actually an indent left by a large TiB precipitate pulled out during tensile test. The second electron (SE) image to the left shows the smoothness of the facet and the BSE image to the right shows the lamellar microstructure underneath. The message conveyed by the images is that debonding occurred at the boride/matrix surfaces and the cracking along the interfaces was not interrupted till to the ends of boride precipitates.

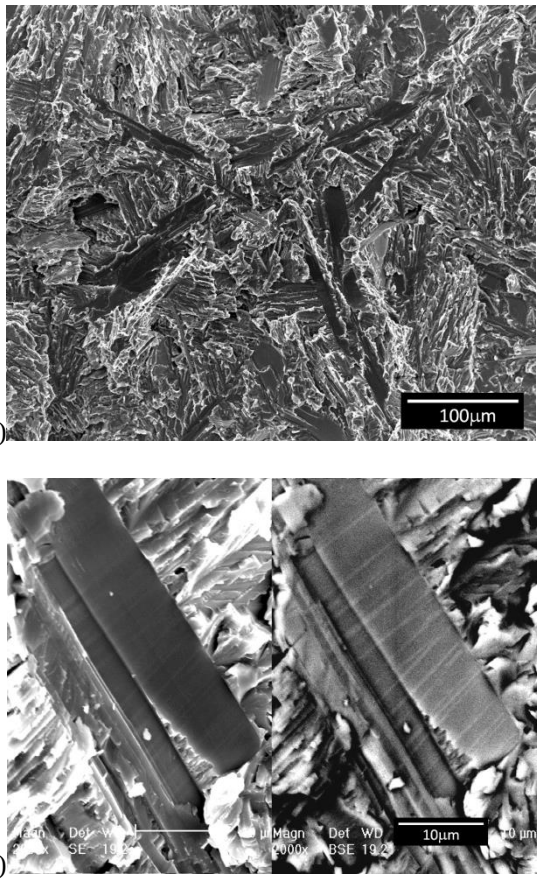

Fig. 12 Fracture surfaces of cast (a) Ti44Al8Nb1B and (b) Ti45Al2Mn4Nb1B.

4.4 Boride related fracture mechanism

The empirical relationship between ductility and lamellar colony size has long been established and it is well known that small lamellar colony size leads to high ductility [3]. However, there is not a clear mechanism to explain it. There were some efforts in the past to characterise the fracture process during tensile testing using acoustic emission to monitor crack initiation [51]. During testing the energy relieved by cracking as acoustic waves was detected by sensors. The location of acoustic events and tensile stress were recorded at the same time. It was found that the first detected cracking occurred at stresses far below the 0.2% proof stress of the alloys. The stress of first cracking was almost right after the proportional limit. That is to say that crack initiation in lamellar microstructures is very easy compared to duplex microstructure where the first cracking was always detected after macro-yielding and just before final fracture. Microstructure examination showed that the cracks were initiated at the lamellar interfaces and grew into the full size of the lamellar colonies immediately. With many cracks inside the material could still be endued with further plastic deformation of up to 1 or 2% (depending on colony size), which manifests that the fracture of lamellar TiAl is crack growth controlled. The acoustic emission study showed that boride precipitates were not related to crack initiation but closely related to crack propagation evidenced by the preference of crack to boride precipitates [51].

Now the lamellar colony size effect can be understood as its ability to limit the early crack size. When the lamellar colony size is smaller than the critical crack size, defined by the fracture toughness of the material, the early cracks will not grow, or need higher stress to grow, and only the early cracks in neighbouring lamellar colonies join together to form cracks longer than the critical crack length, fracture occurs. The role of long boride precipitates is to provide fast crack growth paths along their interfaces to help cracks pass through neighbouring colonies in unfavourable orientations to form long cracks in alloys with small lamellar colonies, as schematically illustrated in Fig. 13. That could be the reason why the ductility was improved once boride precipitate size was reduced by any means [47,48].

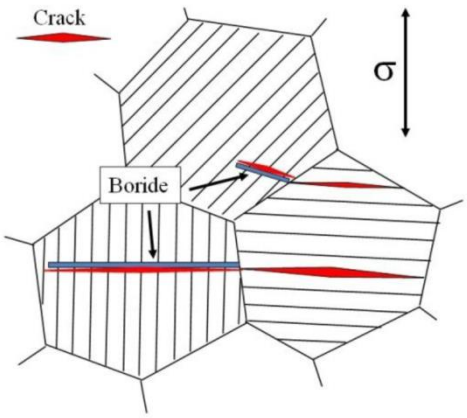

Fig. 13 Schematic illustration showing the role of boride precipitates in the fracture of lamellar TiAl.

5 Boron and thermal/thermomechanical processing

Boron has been used in wrought TiAl alloys for years to improve thermal or thermomechanical processing ability of materials. Most of the TiAl alloys developed early had L + $\beta \rightarrow \alpha$ peritectic reaction solidification paths and a single α phase field. The alloys without boron addition often had coarse columnar structures. These alloys are difficult to forge due to severe surface cracking. Figure 14 shows the surface condition of isothermally forged Ti48Al2Cr2Nb pancake with a starting microstructure shown to the left in Fig. 1. Compared to the Ti48Al2Cr2Nb1B forged pancake the yield of useful material was nearly halved in the boron free alloy. This advantage became less prominent in the wake of newly developed β-solidifying alloys because they always contain enough soft β phase at thermomechanical processing temperatures and fine grains. Nonetheless, a small amount of boron was always added to maximise the potential to reduce grain size before thermomechanical processing.

Fig. 14 Surface conditions of Ti48Al2Cr2Nb(1B) after isothermal forging at 1150°C with 70% reduction in height.

Another benefit brought in by boron addition is the convenience in heat treating hot worked TiAl alloys in the α phase field to obtain fine lamellar microstructures. In boron-free alloys heat treatment time in the α phase field has to be kept at minimum since the fast growth of α grains in this phase field. For example, to obtain fine lamellar colonies in forged Ti46.8Al2.3Nbl.6Cr0.9V the holding time at 1370°C had to be limited to only a few minutes [52]. Some data showed that the α grains in forged Ti48Al2Cr2Nb can grow to 1 mm in 30min at 1400°C whilst the α grain size was kept below 150μm even after 4h at that temperature in forged Ti48Al2Cr2Nb1B [53,54]. This effect can be attributed to Zener pinning of boride particles and a fairly good correlation between α grain size and boride particle spacing was demonstrated in an early publication [55]. In hindsight there is no need for great amount of boron just for grain growth limitation during heat treatment in wrought TiAl alloys. Chan *et al*. heat treated their Ti47Al2Cr2Nb0.2B sheets in α phase field for 1h and still got lamellar colony size of 150μm [56]. Fine dispersive boride precipitates also helped heat treatment of a β-solidifying alloy at temperatures up to 1450°C in the β phase field and still ended with fine microstructures [57]. In this case it took the advantage of boride assisted α transformation during cooling.

Boron was also found beneficial in manufacturing TiAl components with non-conventional processing technologies. Spark plasma sintering (SPS) is a fast processing route to consolidate powders and its application to TiAl powder has been explored for some years [58]. In consolidating Ti47Al2Cr2Nb the maximum temperature had to be limited to below the α transus to prevent excessive grain growth. Thus, only duplex microstructure could be obtained. By adding 0.6% boron into the alloy the maximum processing temperature was raised to above the α transus. With the help of boron precipitates, fine lamellar microstructures were obtained to improve creep resistance [59]. It is the same in hot isostatic pressing (HIPping) TiAl powders. Only in alloys with boron additions could the HIPping temperature be raised to the α phase field, resulting fine lamellar microstructures in the HIPped alloys to reduce sensitivity to defects and improve creep resistance [60,61].

6. Boron-related issues in future alloys development

The future of boron in wrought TiAl alloys seems to be fairly clear: a small addition of boron keeps the starting microstructure fine enough for thermomechanical processing and fine boride precipitates refrain alloys from excessive grain growth during heat treatment. The future work of boron may be mainly related to cast alloys. The development of the TNM alloys was for turbine blade application in PW1000G engine and its family members. PW1000G has an a new geared turbofan engine architecture. It has only 3 stages of low pressure turbine blades but working in much harsher environments than those in the traditional aero-engines such as GEnx. They spin at very high speed and the maximum operation temperature is close to 800°C. Owing to its high efficiency this engine architecture is being adopted by other engine makers for larger engines. Rolls-Royce has announced that its large geared turbofan engine, the UltraFan^{TM}, will be in service in 2025 [62]. If TiAl alloys are used in such engines they

must have 800°C temperature capability. Even though the TNM low pressure turbine blades are manufactured through forging casting is still a processing route worth exploring since the never-ending desire in reducing cost.

The immediate problems facing high temperature TiAl alloys is the creep resistance, especially for enduring applications, and oxidation/corrosion resistance. It is natural to tackle them with alloying of Nb, Ta, Mo or W since they are known to enhance both creep and oxidation/corrosion resistances in TiAl alloys. For cast alloys there is another dimension of difficulties - grain refinement. So far the only reliable way is via boron addition. Combining boron with Ta, W or high concentration of Nb (strong boride formers) leads to formation of titanium monoborides in TiAl alloys, almost irrespective of Al concentration. Larson *et al.* reported early that TiB was the prevalent form in Ti47Al2Cr1Nb0.8Ta0.2W0.15B [63] whilst in low alloying alloys or binary alloys TiB_2 is prevalent in alloys with Al>45% according to the Ti-Al-B liquidus projection diagram created by M.E. Hymen and first quoted in [49]. Titanium monoborides tend to grow to large sizes during casting and have detrimental effects on ductility [47,48]. Thus, their size has to be controlled during casting in order to maintain some ductility which is a challenge in alloys containing those strong boride formers. In addition to size TiB type precipitates are found to form flakes (or curvy borides) more easily than TiB_2 with come alloying species [64]. Flake TiB has been found to reduce ductility in cast Ti44Al4Nb4Hf0.2Si0.45B [47]. The investigation into alloy specie-cooling condition-formation of flake TiB relationship is underway in the IRC.

In the respect of understanding grain refinement mechanisms there are still a few pieces missing. It is still unclear how the fine α grains are formed in the α-solidifying alloys (and beyond) without reactions involving the β phase.

Our understanding of boron in TiAl alloys has been improved with TiAl alloy development. TiAl alloy development will continue for the foreseeable future to cater for new demands inspired by TiAl entering into services. Doubtlessly, boron will accompany TiAl alloys for the new journey ahead.

References:

[1] Bewlay BP, Weimer M, Kelly T, Suzuki A, Subramanian PR. The Science, Technology, and Implementation of TiAl Alloys in Commercial Aircraft Engines. In: MRS Proceedings 1516. Boston; 2013. 49.

[2] Smarsly W, Esslinger J, Clemens H. TiAl for turbine applications – Status and future perspectives, Presentation at GTA 2015, Nanjing; 2015.

[3] Kim Y-W. Ordered intermetallic alloys, part III: gamma titanium aluminides. JOM, 1994;46(July):30.

[4] Larsen DE, Kampe S, Christodoulo L. Effect of XD^{TM} TiB_2 volume fraction on the microstructure of a cast near-gamma titanium aluminide alloy. In: MRS Proceedings 194, 1990. 285.

[5] Kremmer S, Chladil HF, Clemens H, Otto A, Güther V. Near conventional forging of titanium aluminides. In: Ti-2007 Science and Technology. Sendai; 2007. 989.

[6] Larsen DE, Christodoulo L, Kampe S, Sadler P. Investment-cast processing of XD^{TM} near-γ titanium aluminides. Mater. Sci. Eng. A, 1991;A144(1-2):45.

[7] Bryant JD, Christodoulou L, Maisano JR. Effect of TiB_2 additions on the colony size of near gamma titanium aluminides. Scri. Metal. Mater., 1990;24(1):33.

[8] Hu D. Effect of composition on grain refinement in TiAl-based alloys. Intermetallics, 2001;9(12):1037.

[9] Godfrey AB, Loretto MH, The nature of complex precipitates associated with the addition of boron to a γ-based titanium aluminide. Intermetallics, 1996;4(1):47.

[10] Blenkinsop PA, Godfrey AB. Method of adding boron to a heavy metal containing titanium aluminide alloy. US patent; US6488073B1, 2002.

[11] Kartavykh AV, Asnis EA, Piskun NV, Statkevich II, Gorshenkov MV, Tcherdyntsev VV. Lanthanum hexaboride as advanced structural refiner/getter in TiAl-based refractory intermetallics. J. Alloys and Compounds, 2014;588:122.

[12] Yang C, D Hu, A Huang, M Dixon. Solidification and grain refinement in Ti45Al2Mn2Nb1B subjected to fast cooling. Intermetallics, 2013;32:64.

[13] Christodoulou L. Microstructural effects in γ-titanium aluminides; XD TiAl alloys as an example. Presentation in 1st IRC International Gamma TiAl Workshop, Birmingham; 1995.

[14] Shih D, Kim Y-W. Sheet rolling and performance evaluation of beta-gamma (β-γ) alloys. In: Ti-2007 Science and Technology. Sendai; 2007. 1021.

[15] Kremmer S, Chladil HF, Clemens H, Otto A, Güther V. Near conventional forging of titanium aluminides. In: Ti-2007 Science and Technology. Sendai; 2007.989.

[16] Hu D, Jiang H, Wu X. Microstructure and tensile properties of cast Ti-44Al-4Nb-4Hf-0.1Si-0.1B alloy with refined lamellar microstructures. Intermetallics, 2009;17(9):744.

[17] Larson DJ, Liu CT, Miller MK. Boron solubility and boride compositions in $\alpha_2+\gamma$ titanium aluminides. Intermetallics. 1997;5(6):411.

[18] Hecht U, Witusiewicz V, Drevermann A, Zollinger J. Grain refinement by low boron additions in niobium-rich TiAl alloys. Intermetallics, 2008;16(8):969.

[19] Yang C, Jiang H, Hu D, Huang A, Dixon M. Effect of boron concentration on phase transformation texture in as-solidified Ti44Al8NbxB. Scri. Mater., 2012;67(1):85.

[20] Cagran C, Wilthan B, Pottlacher G, Roebuck B, Wickins M, Harding RA. Thermophysical properties of a Ti–44%Al–8%Nb–1%B alloy in the solid and molten states. Intermetallics, 2003;11(11-12):1327.

[21] Witusiewicz VT, Bondar AA, Hecht U, Zollinger J, Artyukh LV, Velikanova TY. The Al–B–Nb–Ti system V. Thermodynamic description of the ternary system Al–B–Ti. J. Alloys and Compounds, 2009;474(1-2):86.

[22] Bermingham MJ, McDonald SD, Dargusch MS, StJohn DH. Grain-refinement mechanisms in titanium alloys. J. Mater. Res., 2008; 23 (1): 97.

[23] Easton M, StJohn DH. Grain Refinement of Aluminum Alloys: Part I. The Nucleant and Solute Paradigms - A Review of the Literature. Metall. Mater. Trans. A, 1999; 30A (June): 1613.

[24] Hu D, Yang C, Huang A, Dixon M, Hecht U. Solidification and grain refinement in Ti45Al2Mn2Nb1B. Intermetallics, 2012; 22:68.

[25] Cheng TT. The mechanism of grain refinement in TiAl alloys by boron addition – an alternative hypothesis. Intermetallics, 2000; 8 (1): 29.

[26] Gosslar D, Hartig Chr, Günther R, Hecht U, Bormann R, Heterogeneous nucleation and growth of the β(Ti) phase in the Ti-Al system – experiments and model calculations. J. Phys.:Condensed Matter, 2009; 21: 464111.

[27] Gosslar D, Günther R, Hecht U, Hartig Chr, Bormann R. Grain refinement of TiAl-based alloys: The role of TiB_2 crystallography and growth. Acta Mater., 2010;58(20):6744.

[28] Inkson BJ, Boothroyd CB, Humphreys CJ. Boron segregation in a (Fe, V, B) TiAl based alloy. Le Journal de Physique IV, 1993;3(C7):397.

[29] Kitkamthorn U, Zhang LC, Aindow M. The structure of ribbon borides in a Ti-44Al-4Nb-4Zr-1B alloy. Intermetallics, 2006;14 (7):759.

[30] Godfrey AB. Grain refinement of a gamma-based titanium aluminide using microalloy additions. Birmingham: University of Birmingham ;1996,1.

[31] Okamoto H. Ti-Al Phase Diagram. J. Phase. Equilibria, 1993;14(1):120.

[32] Imayev RM, Imayev VM, Oehring M, Appel F. Alloy design concept for refined gamma titanium aluminide based alloys. Intermetallics, 2007;15(4):451.

[33] Burgers WG. On the process of transition of the cubic-body-centered modification into the hexagonal-close-packed modification of zirconium. Physica, 1934;1:561.

[34] Hu D, Yang C, Huang A, Dixon M, Hecht U. Grain refinement in beta-solidifying Ti44Al8Nb1B. Intermetallics, 2012;23:49.

[35] Kartavykh AV, Gorshenkov MV, Podgorny DA. Grain refinement mechanism in advanced γ-TiAl boron-alloyed structural intermetallics: The direct observation. Materials Letters, 2015;142:294.

[36] Hu D, Wu X. Tensile ductility of cast TiAl alloys. Materials Science Forum, Vols. 2010;638-642:1336.

[37] Chen CL, Lu W, Lin JP, He LL, Chen GL, Ye HQ. Orientation relationship between TiB precipitate and γ-TiAl phase. Scri. Mater., 2007; 56 (6): 441.

[38] Wang Y, Wang JN, Yang J, Zhang B. Control of a fine-grained microstructure for cast high-Cr TiAl alloys. Mater. Sci. Eng. A, 2005; 392(1-2):235.

[39] Chen GL, Zhang WJ, Liu ZC, Li SL, Kim Y-W. Microstructure and properties of high-Nb containing TiAl-based alloys. In: Gamma Titanium Aluminides 1999. San Diego; 1999.371.

[40] Huang ZW. Inhomogeneous microstructure in highly alloyed cast TiAl-based alloys, caused by microsegregation. Scri. Mater., 2005;52(10):1021.

[41] Hyman ME, McCullough C, Levi CG, Mehrabian R. Evolution of Boride Morphologies in TiAl-B Alloys. Metall. Trans. A, 1991; 22A(July):1647.

[42] Witusiewicz VT, Bondar AA, Hecht U, Velikanova TY. The Al–B–Nb–Ti system IV. Experimental study and thermodynamic re-evaluation of the binary Al–Nb and ternary Al–Nb–Ti systems. J. Alloys Compounds, 2009;472(1-2):133.

[43] Campbell J. Castings. Elsevier Butterworh-Heinemann, Oxford, 2nd edition, 2003, p70.

[44] Zhang J. High Nb content TiAl alloys specified to cast process. Presentation at ISGTA 2014, TMS. San Diego; 2014.

[45] K. Liu, private communication with author, Institute of Metal Research, Chinese Academy of Sciences, October 2005.

[46] Chai LH. private communication with author. Beijing Institute of Technology. 2013.

[47] Hu D. Effect of boron addition on tensile ductility in lamellar TiAl alloys. Intermetallics, 2002;10(9):851.

[48] Hu D, Mei JF, Wickins M, Harding RA. Microstructure and tensile properties of investment

cast Ti-46Al-8Nb-1B alloy. Scr. Mater., 2002;47(4):273.

[49] De Graef M, Löfvander JPA, McCullough C, Levi CG. The evolution of metastable Bf borides in a Ti-Al-B alloy. Acta Metall. Mater., 1992;40(12):3395.

[50] Kartavykh AV, Gorshenkov MV, Podgorny DA. On the state of boride precipitates in grain refined TiAl-based alloys with high Nb content. J. Alloys and Compounds, 2014;586 (S1):S153.

[51] Hu D, Huang A, Jiang H, Mota-Solis N, Wu X. Pre-yielding and pre-yield cracking in TiAl-based alloys. Intermetallics, 2006; 14(1):82.

[52] Chan KS, Kim Y-W. Effects of lamellae spacing and colony size on the fracture resistance of a fully-lamellar TiAl alloy. Acta metal. mater., 1995;43(2):439.

[53] Fuch GE. Homogenization and hot working of Ti-48Al-2Nb-2Cr alloys. In: Structural Intermetallics. Champion; 1993. 193.

[54] Hu D, Blenkinsop PA, Loretto MH. Alpha phase decomposition during continuous cooling in Ti48Al2Cr2Mn with and without boron addition. In: Titaium'99: science and technology. St Petersburg; 1999.290.

[55] Godfrey AB, Hu D, Loretto MH. Thermal stability and properties of lamellar and duplex TiAl-based alloys. In: International symposium on designing, processing and properties of advanced engineering materials. Toyohashi; 1997.37.

[56] Chan KS, Shin DS. Fundamental aspects of fatigue and fracture in a TiAl sheet alloy. Metall. Mater. Trans. A, 1998; 29A (Jan.):73.

[57] Oehring M, Stark A, Paul JDH, Lippmann T, Pyczak F. Microstructural refinement of boron-containing β-solidifying γ-titanium aluminide alloys through heat treatments in the β phase field. Intermetallics, 2013;32:12.

[58] Couret A, Molénat G, Galy J, Thomas M. Microstructures and mechanical properties of TiAl alloys consolidated by spark plasma sintering. Intermetallics, 2008 ;16 (9):1134.

[59] Luo JS, Voisin T, Monchoux JP, Couret A. Refinement of lamellar microstructures by boron incorporation in GE-TiAl alloys processed by Spark Plasma Sintering. Intermetallics, 2013; 36:12.

[60] Habel U, McTiernan BJ. HIP temperature and properties of a gas-atomized γ-titanium aluminide alloy. Intermetallics, 2004 ;12(1):63.

[61] Yang C, Hu D, Wu X, Huang A, Dixon M. Microstructures and tensile properties of hot isostatic pressed Ti4522XD powders. Mate. Sci. Eng. A, 2012;534:268.

[62] "Rolls-Royce shares next generation engine designs" @ http://www.rolls-royce.com/news/press-releases/yr-2014/260214-next-generation.aspx

[63] Larson DJ, Liu CT, Miller MK. The alloying effects of tantalum on the microstructure of an $\alpha_2+\gamma$ titanium aluminide. Mater. Sci. Eng. A, 1999;A270(1),1.

[64] Yang C, Hu D, Wu X, Huang A, Dixon M. The influence of cooling rate and alloy composition on the formation of borides during solidification of boron-containing TiAl alloys. In: Ti-2011. Beijing; 2012.1416.